Published in final edited form as:
Virology. 2011 July 5; 415(2): 83–94. doi:10.1016/j.virol.2011.04.002.

Tyrosine kinase receptor Axl enhances entry of *Zaire ebolavirus* without direct interactions with the viral glycoprotein

Melinda A. Brindley[1,#,‡], **Catherine L. Hunt**[1,‡], **Andrew S. Kondratowicz**[1], **Jill Bowman**[1], **Patrick L. Sinn**[2], **Paul B. McCray Jr.**[2], **Kathrina Quinn**[3], **Melodie L. Weller**[3], **John A. Chiorini**[3], and **Wendy Maury**[1,*]

[1] Department of Microbiology, University of Iowa, Iowa City, IA 52242

[2] Department of Pediatrics, University of Iowa, Iowa City, IA 52242

[3] Molecular Physiology and Therapeutics Branch, National Dental and Craniofacial Research Branch, National Institutes of Health, Bethesda, MD 20892

Abstract

In a bioinformatics-based screen for cellular genes that enhance *Zaire ebolavirus* (ZEBOV) transduction, *AXL* mRNA expression strongly correlated with ZEBOV infection. A series of cell lines and primary cells were identified that require Axl for optimal ZEBOV entry. Using one of these cell lines, we identified ZEBOV entry events that are Axl-dependent. Interactions between ZEBOV-GP and the Axl ectodomain were not detected in immunoprecipitations and reduction of surface expressed Axl by RNAi did not alter ZEBOV-GP binding, providing evidence that Axl does not serve as a receptor for the virus. However, RNAi knock down of Axl reduced ZEBOV pseudovirion internalization and α-Axl antisera inhibited pseudovirion fusion with cellular membranes. Consistent with the importance of Axl for ZEBOV transduction, Axl transiently co-localized on the surface of cells with ZEBOV virus particles and was internalized during virion transduction. In total, these findings indicate that endosomal uptake of filoviruses is facilitated by Axl.

Keywords

Axl; filovirus; Ebolavirus; Marburgvirus; virus entry; tyrosine kinase receptors

Introduction

The filoviruses *Ebolavirus* and *Marburgvirus* (MARV) have caused a number of devastating hemorrhagic fever outbreaks in Africa over the past thirty years. These enveloped, non-segmented, negative-stranded RNA viruses are listed as a Category A biodefense agents due to the significant mortality associated with infection. No vaccines or antiviral therapies are

[*]Corresponding author: Wendy Maury, 3-750 Bowen Science Building, Department of Microbiology, University of Iowa, Iowa City, IA 52242 USA, 1 319 335 8021(office); 1 319 335 9006 (fax), wendy-maury@uiowa.edu.
[‡]Authors contributed equally to this work.
[#]**Current address:** Department of Pediatrics, Emory University School of Medicine and Children's Healthcare of Atlanta, Atlanta, Georgia 303221

currently available against these viruses. A better understanding the cellular proteins that are required for filoviruses entry into cells may lead to strategies to combat these pathogens.

The *Zaire ebolavirus* (ZEBOV) and *Lake Victoria marburgvirus* (MARV) glycoproteins (GP) facilitate pseudovirus entry into a broad range of cell types from many mammalian species (Wool-Lewis and Bates, 1998). This wide tropism has complicated the identification of cellular proteins required for filovirus entry. Nonetheless, several different plasma membrane associated proteins have been identified to enhance filovirus infection/transduction. The C type lectins have been shown to increase entry into some cells (Alvarez et al., 2002; Baribaud et al., 2002; Geijtenbeek and van Kooyk, 2003; Lasala et al., 2003; Lin et al., 2003; Marzi et al., 2004; Simmons et al., 2003a; Takada et al., 2004), but many highly permissive cells do not contain C type lectins leading investigators to conclude that this group of plasma membrane-associated proteins serve as adherence factors rather than receptors that mediate virus entry. Folate receptor-α was identified to enhance ZEBOV-GP pseudovirion entry when the protein was ectopically expressed in Jurkat cells (Chan et al., 2001); however, this protein was subsequently shown to be unnecessary in a number of permissive cells (Simmons et al., 2003b; Sinn et al., 2003). Most recently, the tyrosine kinase receptor Axl was identified to facilitate ZEBOV and MARV transduction of some but not all permissive cell lines (Shimojima et al., 2007; Shimojima et al., 2006).

Axl is one of three members of the TAM (Tyro3, Axl, Mer) protein family (Linger et al., 2008). These proteins are single pass, type 1 plasma membrane-associated proteins. The ectodomain consists of two immunoglobulin-like domains as well as and two fibronectin-like domains (Linger et al., 2008). The two immunoglobulin-like domains are responsible for TAM family interactions with three known ligands or groups of ligands, the Tubby family of proteins, Gas6 and Protein S (Caberoy et al., 2010; Heiring et al., 2004; Sasaki et al., 2006; Stitt et al., 1995; Varnum et al., 1995). These ligand/Axl interactions lead to receptor homo- and heterodimerization of Axl, Mer and Tyro3 and subsequent tyrosine-dependent signaling. Specifically, Gas6/Axl ligation results in a variety of cell type-dependent effects including cell migration/chemotaxis (Fridell et al., 1998; Zhang et al., 2008), adhesion (McCloskey et al., 1997), cell survival (Zheng et al., 2009) and division (Lee et al., 1999).

While no direct interactions between ZEBOV-GP pseudovirions and Axl have been demonstrated, site-directed mutagenesis of Axl identified residues in both the ectodomain and the cytoplasmic tail that are required for enhanced ZEBOV-GP pseudovirion transduction (Shimojima et al., 2007). The requirement of Axl cytoplasmic tail residues suggests Axl signaling may be involved in Axl-dependent ZEBOV-GP transduction. We recently demonstrated that Axl enhances bulk fluid phase uptake or macropinocytosis of cargo as diverse as 70 kDa dextran, ZEBOV-GP pseudovirions, ZEBOV virus-like particles (VLPs) and infectious ZEBOV. Axl-dependent macropinocytosis required actin polymerization and was profoundly inhibited by the amiloride analog EIPA (Hunt et al., 2011).

In a large screen of human tumor cell lines that correlated cellular gene expression with ZEBOV-GP pseudovirion transduction, we found that Axl expression positively correlated with ZEBOV-GP-dependent transduction, but not VSV-G-dependent. To better understand the role of Axl in filovirus entry, we identified steps involved with ZEBOV-GP-dependent transduction that require Axl expression. Our findings indicate that Axl does not directly interact with ZEBOV-GP, but instead facilitates filovirus internalization and membrane fusion, consistent with a newly appreciated role of Axl in macropinocytosis.

Results

AXL mRNA expression correlates with ZEBOV-GP-mediated transduction of the NCI-60 panel of human tumor cells

To identify proteins important for ZEBOV-GP-mediated entry, we performed Gene Correlation Analyses (CGA) using the NCI-60 panel of human tumor cells. CGA screens have previously identified cellular receptors for adeno associated virus 5 and 6 and implicated the GTPase RhoC with enhancing both ZEBOV and VSV transduction (Di Pasquale et al., 2003; Quinn et al., 2009b; Weller et al., 2010). This bioinformatics-based approach correlated virus transduction with gene expression in the NCI-60 cell panel. VSV/EGFP virions pseudotyped with either mucin domain deleted ZEBOV glycoprotein (ZEBOV-GP ΔO VSV) or VSV-G (VSV-G VSV) were transduced into 52 of the NCI-60 cell lines. ZEBOV-GP ΔO that has the mucin domain of the glycoprotein deleted was used in this screen and most of the other experiments in this study because it contains the intact viral glycoprotein receptor binding domain, confers entry in a manner similar to the full-length glycoprotein, but produce titers that are consistently higher (Jeffers et al., 2002).

The relative mean transduction values of three independent experiments were used as a seed file and compared with gene array data from the NCI-60 panel that is publically available at http://dtp.nci.nih.gov/compare/. Using a Pearson correlation analysis, a list of cellular genes that strongly and positively correlated with ZEBOV-GP-dependent transduction was generated. The initial list of genes whose expression was associated with ZEBOV-GP ΔO VSV transduction with a highly positive Pearson correlation coefficient (PCC) was further delimited using EnTuned software to identify function, subcellular location, and pathway associations since we were interested in genes that expressed plasma membrane associated proteins (http://www.macresearch.org/entuned_pl). Additionally, genes that highly correlated with transduction of both ZEBOV-GP and VSV-G pseudovirions were discarded under the assumption that these genes encoded proteins involved in VSV uncoating and/or expression and were not genes directly pertinent to ZEBOV-GP-dependent entry.

A number of genes were identified that encoded plasma membrane-associated proteins that correlated with ZEBOV-GP pseudovirion transduction, but did not correlate with VSV-G pseudovirion transduction. Expression of one gene that correlated strongly was the Tyro3/Axl/Mer (TAM) family member *AXL* (Fig. 1A). ZEBOV-GP-dependent transduction of the cell panel, but not VSV-G-dependent transduction demonstrated a similar trend to that observed with *AXL* mRNA expression (Fig. 1B and C). *AXL* mRNA expression in the NCI-60 panel correlated with ZEBOV-GP-mediated transduction with a PCC of 0.517 that was found to be highly statistically significant ($p < 0.001$). Axl had been previously identified to facilitate filovirus entry in a cDNA screen performed by Shimojima, et al (Shimojima et al., 2006). While Shimojima et al. demonstrated that the other two TAM family members Dtk (also called Tyro3) and Mer can also enhance ZEBOV-GP dependent transduction into poorly permissive cells (Shimojima et al., 2006), neither Dtk nor Mer positively correlated with ZEBOV-GP-dependent transduction in our screen. Interestingly, other proteins such as folate receptor-α or C type lectins that are implicated in filovirus attachment and entry also did not correlate with ZEBOV-GP-dependent transduction in this screen. Since C type lectins, DC SIGN, DC SIGNR, LSECtin and mannose binding lectin, are primarily or exclusively expressed on hematopoietic and/or endothelial cells (Allavena et al., 2004; Geijtenbeek and Gringhuis, 2009; Kerrigan and Brown, 2010; Simmons et al., 2003a), this finding is not unexpected as the NCI-60 panel is principally composed of other cells types.

To validate the NCI-60 microarray correlation findings, we initially evaluated cell surface expression of Axl on two of the cell lines identified by the gene array to have high *AXL*

mRNA expression and two lines with low *AXL* mRNA expression. Axl protein expression levels as assessed by binding of polyclonal antisera directed against the Axl ectodomain to live cells in a flow cytometric assay were consistent with the microarray data. M14 and UACC257 (#3 and #7 melanoma lines in Fig. 1, respectively) that had little or no *AXL* mRNA expression did not have detectable Axl on their surface (Fig. 2A). In contrast, SNB-19 and SN12C (#4 CNS line and #6 renal line in Fig. 1) that had abundant *AXL* mRNA expression in the gene array expressed large quantities of cell surface Axl (Fig. 2B). Evaluation of Axl surface expression on other NCI-60 lines was also consistent with the gene array results (data not shown). To further appraise Axl expression on primary cell populations, human foreskin fibroblasts (Hff) and human umbilical vein endothelial cells (HuVEC) were examined and found to express readily detectable levels of cell surface Axl (Fig. 2C). These same six cell populations were also assessed for both Dtk and Mer expression and none of them was found to express the other two TAM family members (data not shown).

Axl enhancement of ZEBOV-GP-mediated infection is cell type-specific

To examine the requirement for Axl in ZEBOV-GP-mediated entry, we utilized polyclonal antisera directed against the Axl ectodomain that has been shown to inhibit ZEBOV-GP-dependent transduction in some cells (Shimojima et al., 2006). VSV-G pseudovirions served as controls in these studies since Axl expression did not positively correlate with VSV-G-dependent transduction in our CGA. We used Vero and 293T cells that do not require Axl expression for optimal ZEBOV pseudovirion transduction as negative controls in this study (Shimojima et al., 2006). As previously demonstrated (Shimojima et al., 2006), we found that 293T cells do not express Axl, whereas Vero cells express significant levels of surface Axl, but Axl expression has no effect on ZEBOV transduction (data not shown). In addition to transducing these cells, we extended our studies to include two Axl-expressing lines from the NCI-60 panel as well as our Axl-expressing primary cells (Hffs and HuVECs). Cells were incubated with Axl antisera or normal goat sera (GS) and transduced with equivalent amounts of ZEBOV-GP ΔO or VSV-G VSV pseudovirions. Axl antisera significantly reduced ZEBOV-GP-dependent transduction of SNB-19, Hff, and HuVECs, but did not decrease transduction of 293T, Vero or SN12C cells (Fig. 3A). Thus, ZEBOV transduction was enhanced by surface availability of Axl in three of the Axl-expressing cell populations. Additionally, our findings with Vero and SN12C cells are consistent with the previous report that surface Axl expression does not predict that Axl will facilitate ZEBOV-GP-dependent uptake (Shimojima et al., 2006). Similar findings using Axl antisera incubated with these different cell populations were also observed with FIV pseudovirions bearing ZEBOV GP (data not shown). This highlights the fact that the effect of Axl on ZEBOV transduction was independent of the viral core particle used. As a result of this consistent finding, we used both VSV and FIV pseudovirion in this study and some of the studies reported here were performed with FIV pseudovirions, whereas others used VSV pseudovirions.

Surprisingly, we found that VSV-G transduction into SN12C, Hffs and HuVECS was decreased by Axl antibodies. SNB-19 cells that had reduced ZEBOV-GP-dependent entry in the presence of Axl antisera did not have reduced VSV-G transduction in the presence of the antisera. This finding is consistent with our previously published studies using RNAi knock down of Axl (Hunt et al., 2011). Interestingly, both ZEBOV-GP- and VSV-G-dependent entry were inhibited by anti-Axl antibodies in the primary cell populations.

Enhancement of ZEBOV transduction by surface expression of Axl

We recently showed that RNAi knock down of endogenous *AXL* expression reduced replication of infectious ZEBOV by 80% during a 20 hour virus infection, directly

demonstrating the importance of Axl for optimal ZEBOV entry into some cells (Hunt et al., 2011). As these initial studies only evaluated ZEBOV infection during a single round of infection, we sought to determine if Axl antisera effectively decreased ZEBOV infection over a longer term infection. In these studies, a recombinant, infectious VSV that has the G gene replaced with ZEBOV-GP ΔO and EGFP (ZEBOV-GP-VSV/EGFP) that allowed us to assess virus replication under BSL2 conditions. These studies were performed in SNB-19 cells that are part of the NCI-60 panel (CNS cell line #4, Fig. 1) and served a model cell type that requires Axl for optimal ZEBOV GP transduction, but not VSV-G transduction. These cells express large quantities of Axl and can be readily transfected, providing an excellent cell line for understanding the role of Axl in ZEBOV infection. Axl antisera or GS was added 15 minutes prior to the addition of infectious ZEBOV-GP-VSV/EGFP (MOI= 0.1). EGFP positive cells in the cultures were assessed by flow cytometry at days 1–4 of infection. Axl antisera decreased the number of VSV infected cells at days 2 and 3, indicating reduced levels of initial infection and delayed spread of the virus (Fig. 3B). Thus, consistent with our earlier study (Hunt et al., 2011), loss of Axl availability on the surface of SNB-19 cells using Axl-antisera also inhibits ZEBOV-GP-dependent infection.

Previously, it has been shown that expression of Axl and other TAM family members enhanced the entry of ZEBOV into cells that were normally not permissive to ZEBOV (Shimojima et al., 2006). We thus sought to determine if expression of Axl could enhance ZEBOV-GP-mediated entry into additional cell populations identified in our current CGA screen as low Axl mRNA expressers and poorly permissive for ZEBOV transduction. We transfected two NCI-60 NSCLC populations, NCI-H460 and NCI-H522 (NSCLC cell lines #8 and 9, respectively, Fig. 1), with an empty expression vector or with an expression vector bearing Axl (Fig. 3C). Flow cytometric analysis of the transfected cells demonstrated cell surface expression of Axl in the Axl plasmid transfected populations (data not shown). Cells were transduced with ZEBOV-GP ΔO or VSV-G VSV (MOI=0.005) at 48 hours following transfection. The ratio of transduction in the presence of empty plasmid versus the Axl expressing vector was then calculated after live cell assessment for EGFP by flow cytometry. A 3.5 fold increase in ZEBOV-GP-mediated transduction was observed in the NCI-H522 cells (Fig. 3C) whereas a more modest 1.7 fold increase was observed in NCI-H460 cells (data not shown). Transduction ratios of VSV-G VSV remained unchanged in both cell populations, indicating that transient expression of Axl in cells that do not normally express abundant levels of Axl allows for a specific enhancement of ZEBOV-GP-mediated entry.

Transduction of proteolytically processed ZEBOV pseudovirion requires Axl

Proteolytic processing of ZEBOV-GP1 is required for virion fusion to occur (Chandran et al., 2005; Schornberg et al., 2006). We inquired if the requirement for Axl for optimal ZEBOV transduction into SNB-19 cells was affected by proteolytic processing of ZEBOV-GP pseudovirions. We transfected SNB-19 cells with either *AXL* RNAi or an irrelevant RNAi and transduced either full length or thermolysin-treated full length ZEBOV-GP VSV into the transfected cells. The ZEBOV-GP on virions mock or thermolysin-treated was immunoblotted to verify protease cleavage of the viral glycoprotein (Supplemental Fig. 1). *AXL* RNAi decreased the total amount of Axl protein present in SNB-19 cell lysates and reduced Axl on the surface of cells (Fig. 4A and B). As previously observed by others (Schornberg et al., 2006), thermolysin-treated virions had about four fold higher transduction that virions pseudotyped with untreated, full length ZEBOV-GP. However, transduction into *AXL* RNAi-treated cells of either untreated or thermolysin-treated virions was reduced by approximately 55% indicating that the thermolysin-treated virions still required Axl for optimal transduction into SNB-19 cells (Fig. 4C).

ZEBOV-GP does not interact with the Axl ectodomain

Evidence demonstrated a requirement for Axl in some cells for optimal filovirus transduction, but direct interaction of ZEBOV-GP and Axl has not been shown. Co-immunoprecipitations (co-IPs) between Axl and ZEBOV-GP were performed to determine if we could detect direct interactions between the two proteins. The chimeric protein Axl-Fc was bound to Protein A beads and incubated with ZEBOV-GP ΔO pseudotyped FIV, baculovirus GP64 pseudotyped FIV or the endogenous Axl ligand Gas6. Neither of the two viral glycoproteins interacted with Axl-Fc (Fig. 5A); however, Gas6 bound to Axl-Fc indicating the immunoprecipitation conditions were appropriate for detection of ligand-receptor interactions.

To further explore possible interactions between ZEBOV-GP and Axl, co-IPs were repeated to determine if ZEBOV-GP pseudotyped virus could pull-down Axl from SNB-19 cell lysates. ZEBOV-GP ΔO pseudotyped FIV particles were bound to beads using anti-GP1 antibodies. SNB-19 cell lysates were incubated with the beads and bound proteins were identified by immunoblotting. Again, ZEBOV-GP failed to pull-down Axl from the cell lysates (Fig. 5B). As a cellular receptor for ZEBOV has yet to be identified, we were unable to provide a positive control for ZEBOV-GP co-immunoprecipitations in this study.

We also evaluated possible interactions of thermolysin-cleaved ZEBOV-GP with Axl. We verified that thermolysin treatment of virions produced the 19 kDa GP1 product (Supplemental Figure 1) and evaluated viral particles for their ability to interact with Axl-Fc during a co-IP (Fig. 5C). Pre-cleaved virions also failed to interact with Axl. These studies provide a number of lines of evidence that ZEBOV-GP and Axl do not interact under the conditions tested.

Loss of Axl does not affect ZEBOV pseudovirion binding to SNB-19 cells, but decreases ZEBOV-GP pseudovirion internalization and fusion

We could not detect direct interactions between Axl and ZEBOV-GP in pull downs; however, we also assessed Axl/ZEBOV-GP interactions by evaluating if loss of cell surface availability of Axl impacted ZEBOV-GP pseudovirion binding to SNB-19 cells. We first tested whether pre-incubation of commercially available, purified Axl-Fc (R&D Systems) with SNB-19 or 293T cells reduced EBOV transduction and found that this had no effect on transduction of either ZEBOV-GP ΔO or VSV-G VSV pseudovirion transduction into either cell type (Fig. 6A). In these studies, we used 293T cells as a negative control since Axl is not expressed in these cells. *AXL* RNAi knock down of Axl expression also had no effect on ZEBOV-GP ΔO FIV pseudovirion binding to SNB-19 cells (Fig. 6B). Finally, pre-treatment of SNB-19 cells with polyclonal Axl antisera and subsequent incubation with ZEBOV-GP ΔO or VSV-G VSV did not reduce ZEBOV-GP ΔO or VSV-G pseudovirion binding to cells (data not shown). In total, our data provide no evidence that Axl directly interacts with ZEBOV-GP. Thus, it is unlikely that Axl serves as a cellular receptor for this virus.

We also determined if RNAi knock down of *AXL* inhibited ZEBOV-GP pseudovirion internalization. We treated cells with *AXL* RNAi or an irrelevant RNAi (Block-It, Invitrogen) and, forty-eight hours later, ZEBOV-GP ΔO or VSV-G FIV pseudovirions were bound to SNB-19 cells for 1 hour at 4°C. The cells were washed to remove unbound virus. Under these conditions where no virions are internalized into cells, detection of cell-bound virions was completely abrogated by trypsin treatment (data not shown). Following a two hour incubation of these virus-bound cells at 37°C, cells were treated with trypsin to remove any virions that were not internalized, washed with PBS with 5% FCS and lysed. Lysates were immunoblotted for FIV capsid and cellular actin and the amount of the proteins was quantified by ECL photon emission on the immunoblot. Amount of internalized virus was

normalized to cell numbers using cellular actin signals. The data are shown as the amount of internalized virions in the presence of *AXL* RNAi divided the amount of internalized virions in cells treated with Block-It (Fig. 6C). We found that ZEBOV-GP ΔO pseudovirion internalization was reduced approximately 40% by *AXL* RNAi treatment, whereas providing our first evidence that post-binding entry steps of ZEBOV are affected by Axl. Similar studies with VSV-G pseudovirions demonstrated that Axl knock down had no effect on internalization of these virions.

To further explore the effect(s) of Axl on ZEBOV-GP-mediated post-binding events, we assessed virion/endosomal membrane fusion using ZEBOV-GP ΔO bearing virus like particles (ZEBOV ΔO VLPs). As virion fusion events are downstream from virion internalization events, we predicted that Axl antisera would also reduce fusion. ZEBOV ΔO VLPs were generated containing recombinant Src/β-lactamase protein as previously described (Quinn, 2009) and were used in these studies to complement our internalization findings using FIV cores rather than ZEBOV cores. In this assay, β-lactamase activity was detected by pre-loading the fluorescent β-lactam substrate CCF2/AM into the cytoplasm of SNB-19 cells. ZEBOV ΔO VLP fusion with endosomal membranes was measured by a change in fluorescence due to cleavage of the β-lactam ring (Cavrois et al., 2002; Cavrois et al., 2004). In a manner consistent with our FIV-based internalization assays, the addition of anti-Axl antisera decreased ZEBOV ΔO VLP fusion by about 40% compared to the normal GS (Fig. 6D). Thus, both virus internalization and fusion was reduced by the loss of available surface expressed Axl, indicating that Axl is involved in ZEBOV-GP-mediated entry at a post-binding step.

Axl internalizes as ZEBOV pseudovirions enter SNB-19 cells

To determine the localization of Axl during ZEBOV-GP ΔO pseudovirions entry, both pseudovirions and Axl were tracked in SNB-19 cells over a 45 minute time course of ZEBOV-GP ΔO FIV transduction using confocal microscopy. Axl was found to be present primarily on the surface of naive SNB-19 cells (data not shown). A similar distribution of Axl was observed in cells that were cooled to 4°C and incubated for 60 minutes with either ZEBOV-GP ΔO FIV (MOI=250) (Fig. 7A and 8A) or FIV-VSV-G (MOI=250) (Supplemental Figure 2). A high MOI was used in these studies to allow good confocal detection of virions using an anti-FIV capsid antibody. Cell surface co-localization of EBOV pseudovirions and Axl was evident during the initial 4°C binding step in both permeabilized and non-permeabilized cells (Fig. 7A and 8A). Following this one hour binding step, unbound virus was removed and cells were shifted to 37°C for various times (Fig. 7B–D and 8B–D). At 15 minutes following the temperature shift, both Axl and ZEBOV-GP ΔO FIV pseudovirions remained almost exclusively on the cell surface and frequent co-localization was still observed. By 30 minutes, both virions and Axl appeared to be internalized since decreased FIV capsid and Axl signals were consistently observed in non-permeabilized cells (Fig. 8C) and, in the permeabilized cells, expression of both antigens appeared distributed throughout the cell (Fig. 7C). At 30 to 45 minutes, little co-localization of the two signals occurred and, by 45 minutes, while much of the Axl remained intracellular, a portion of Axl appeared to be surface expressed again, suggesting the possibility that some was recycled to the surface of the cells (Fig. 7D and 8D). Combined, these studies provide evidence of internalization of both virions and Axl during virion infection, although co-localization of the two signals within cells did not occur.

Parallel confocal microscopy studies were performed with SNB-19 cells incubated with FIV virions pseudotyped with no viral glycoprotein and FIV virions pseudotyped with VSV-G. Axl and non-enveloped virions did not co-localize under these conditions at any time, and as expected, were unable to enter the cells at any point (data not shown). Surprisingly, we observed co-localization of VSV-G pseudovirions and Axl on the surface of cells at the zero

time point. Much of this co-localization of the two signals was lost by 15 minutes at 37°C (Supplementary Figure 2). Unlike the EBOV GP pseudovirion studies, s virions became intra-cellular over the 45 minutes, a parallel internalization of Axl was not observed. Instead, Axl remained primarily cell surface associated, suggesting that Axl was not internalized with the VSV-G pseudovirions.

Discussion

In a bioinformatics-based screen using a large panel of human tumor cells, Axl expression strongly correlated with ZEBOV-GP pseudovirion transduction. Axl was previously characterized to enhance filovirus entry into some cell populations (Shimojima et al., 2006) and, in a similar manner, we also observed that surface expression of Axl enhances ZEBOV pseudovirion entry into some cells. Using multiple approaches to inhibit Axl, we provided evidence that ZEBOV pseudovirion internalization and subsequent fusion is inhibited by loss of surface Axl expression. The impact on virus internalization did not appear to be due to direct Axl interaction with ZEBOV-GP pseudovirions or reduced ability of ZEBOV pseudovirions to interact with permissive cells, suggesting that Axl was stimulating ZEBOV-GP pseudovirion uptake through indirect mechanisms rather than serving as a receptor for ZEBOV. Consistent with a role for Axl in ZEBOV internalization, Axl and virions concomitantly internalized during pseudovirion entry.

Both ZEBOV pseudovirion internalization and membrane fusion were decreased by about 40% with the reduction of Axl on the surface of SNB-19 cells as assessed by *AXL* RNAi and Axl-specific antisera using two different virion model systems (Fig. 6C–D). As the effect on both of these steps results in a similar level of inhibition, it is likely that the effect occurs at the upstream event, internalization, and that fusion is affected as a result of reduced internalization. The modest impact on both of these entry events was associated with significantly decreased/delayed virus replication using a single administration of Axl antisera prior to initiation of infection (Fig. 3B). It is surprising that a 40% decrease in these entry events resulted in a complete loss of detectable infection at two days following infection. One possible explanation is that additional steps in virus replication that were not evaluated in these studies are inhibited by loss of cell surface Axl in addition to virus internalization.

We recently demonstrated that Axl stimulates bulk fluid phase uptake or macropinocytosis (Hunt et al., 2011). Loss of Axl-dependent macropinocytic activity resulted in not only decreased uptake of ZEBOV pseudovirions, but other cargos such as large molecular weight dextran. Thus, we propose that greater numbers of ZEBOV particles bound to or in proximity with the surface of SNB-19 cells are internalized into endosomes due to Axl-dependent macropinocytosis, resulting in higher levels of virus infectivity. While our studies indicated that Axl-dependent macropinocytosis is important for enhanced ZEBOV entry (Hunt et al., 2011), the trigger(s) that stimulate macropinocytosis have yet to be identified.

Several lines of evidence suggest that cell signaling pathways are activated during Axl-dependent enhancement of ZEBOV-GP-mediated transduction. Shimojima et al. demonstrated that deletions in the cytoplasmic tail of Axl reduced Axl-mediated enhancement of ZEBOV-GP pseudovirion transduction, arguing that cell signaling is critical for Axl-enhanced ZEBOV infection (Shimojima et al., 2007). Our studies demonstrated that phospholipase C inhibitors specifically inhibited ZEBOV pseudovirion transduction in Axl-dependent cells, but not in cells where Axl does not enhance ZEBOV transduction (Hunt et al., 2011).

Signaling through Axl activation has been almost exclusively studied using the endogenous Axl ligand Gas6. Gas6 binding to Axl leads to a variety of cell-dependent biological outcomes including cytoskeleton rearrangements, cell migration, cell survival and division (Demarchi et al., 2001; Goruppi et al., 2001; Goruppi et al., 1997, 1999; Melaragno et al., 2004; Nielsen-Preiss et al., 2007; Zheng et al., 2009). Prior to our study (Hunt et al., 2011), a role for Axl in macropinocytosis had not been appreciated; however, TAM family member Mer is known to activate phagocytosis in macrophages (Scott et al., 2001; Shao et al., 2009). While co-IPs have demonstrated that the phosphorylated tyrosines in the cytoplasmic tail of TAM proteins interacts with p85alpha and p85beta subunits of PI3K, PLCγ, RanBPM, Grb2 and Src (Braunger et al., 1997; Hafizi et al., 2005), Gas6/Axl interactions have only been shown to result in signaling through PI3K, Src and Grb2 (Demarchi et al., 2001; Goruppi et al., 2001; Goruppi et al., 1997, 1999; Lee et al., 1999; Melaragno et al., 2004; Son et al., 2007; Weinger et al., 2008; Wilhelm et al., 2008; Zheng et al., 2009). As stimulation of Axl-dependent macropinocytosis that enhanced ZEBOV infection did not require activation of the PI3K/Akt pathway, but phospholipase C-dependent pathways (Hunt et al., 2011), Axl signaling appears to occur through at least two different signaling pathways, leading to different physiological consequences. Recently, a new group of ligands for the TAM family kinases was identified (Caberoy et al., 2010). The Tubby protein interacts only with Mer, whereas tubby-like protein1 (Tulp1) interacts with all three TAM family members. Tubby contain elements that are essential for Mer binding, phosphorylation and phagocytosis activation. Tulp1 contains all of these functional elements as well, and is capable of binding to Axl *in vitro*. Additionally, activation of PLCγ and PLCβ has been linked to Tubby protein activation (Carroll et al., 2004). However, it is not clear whether Tulp1 binding to Axl activates Axl signaling and is the ligand responsible for Axl-induced macropinocytosis. Further, it is not known if Tulp1/Axl interactions lead to PLC activation or whether other downstream signaling is activated by this interaction. While it is enticing to speculate that Tulp1 may be activating Axl and thereby stimulating macropinocytosis, this has yet to be directly demonstrated.

While recent studies suggest that a novel ligand may be responsible for activating Axl-dependent macropinocytosis leading to increased uptake of ZEBOV, an alternative Axl interaction may also stimulate ZEBOV entry. The Axl ectodomain is known to heterodimerize with IL-15-bound IL-15 receptor leading to active Axl signaling (Budagian et al., 2005). Thus, it is also possible that ZEBOV-GP may stimulate Axl signaling events as a result of binding to a currently unidentified receptor that in turn heterodimerizes with Axl. Such interactions may lead to activation of downstream signaling pathways. Such a model would also be consistent with a role for Axl in ZEBOV virion internalization.

As Shimojima et al. have shown (Shimojima et al., 2006), we observed that Axl enhances ZEBOV-GP-dependent transduction in some cells, but not others. While some cells such as 293T cells do not express Axl, other cells such do express Axl, but expression of the protein does not enhance ZEBOV entry. Cell lines such as VeroE6 (Shimojima et al., 2006), Vero and SN12C express Axl on their plasma membrane, but Axl expression does not affect ZEBOV-GP-dependent transduction of these cells. It is possible that pathways connecting Axl to macropinocytosis may be disrupted in these transformed cell lines. In contrast, other Axl-expressing cells such as SNB-19 cells that have roughly equivalent levels of surface-expressed Axl as SN12C cells have a strong dependence upon Axl for optimal ZEBOV-GP-mediated transduction. Thus, the transduction requirement for Axl in each permissive cell population needs to be empirically determined. We also demonstrated here that in two primary human cell populations (Hffs and HuVECs), optimal ZEBOV-GP-mediated transduction requires Axl. These initial studies with primary cell populations suggest the possibility that Axl may be important for *in vivo* filoviral infection and pathogenesis.

As proteolytic cleavage of ZEBOV-GP might abrogate the need for Axl, we investigated the effect of thermolysin cleavage of GP1 on the requirement of Axl (Fig. 4C). We found that while virions that were protease pre-treated had higher levels of transduction, entry of these particles was just as sensitive to the loss of Axl as particles containing full length ZEBOV-GP. Thus, we concluded that the requirement for Axl is independent of requisite proteolytic pathways needed for productive ZEBOV transduction.

In our initial assessment of filovirus transduction of Axl-expressing cells, VSV-G pseudotyped virions were used as a negative control. Unexpectedly, VSV-G-dependent entry into some cells was reduced about two-fold by Axl antisera (Fig. 3A). This was a more modest impact than that observed for ZEBOV-GP transduction, but statistically significant. This finding provides additional evidence that the involvement of Axl in ZEBOV-GP-mediated entry is likely to due to indirect interactions with the virions rather than direct viral glycoprotein/receptor interactions. Even more surprising was our observation that some cells that required Axl for ZEBOV-GP-dependent entry did not require it for VSV-G-dependent entry and, conversely, other cell lines required Axl for VSV-G-dependent entry but not uptake mediated by ZEBOV-GP. One possible explanation for this finding is that uptake pathways utilized by these viruses may differ in these various cells. As we have demonstrated that Axl expression enhances macropinocytosis, but not other uptake pathways (Hunt, et al. 2011), we would propose that macropinocytosis also mediates VSV-G-dependent uptake into some cells. Consistent with the possibility, Bhattacharyya et al. demonstrated that VSV-G entry into some cells does not utilize clathrin coated pits, a entry pathway that has been well established for VSV-G entry into many cells (Bhattacharyya et al., 2010). Of note, entry of both pseudovirions into the primary cells, Hffs and HuVECs, was enhanced by Axl expression. Therefore, further exploration of uptake mechanisms of these viruses in other relevant primary cells such as macrophages and dendritic cells is warranted.

Material and Methods

Cell lines

Cell lines from the NCI-60 panel (dtp.nci.nih.gov/docs/misc/common_files/cell_list.html) were examined for their ability to support mucin domain deleted ZEBOV-GP (ZEBOV-GP ΔO) pseudovirion transduction. All NCI-60 cells were maintained in RPMI with 5% FCS and pen/strep. Human umbilical vein endothelial (HuVEC) cells were isolated from a fresh umbilical cord and maintained in EBM media (Lonza/Cambrex) supplemented with the EBM bullet kit. Human foreskin fibroblasts (Hffs) (ATCC, CRL-1635) were grown in DMEM with 15% FCS and pen/strep.

Antibodies and Fc molecules

Antibodies were purchased commercially when possible. These included goat anti-Axl (#AF154, R&D Systems), goat anti-VSV-G (#A190-130A, Bethyl Labs), mouse anti-human β-tubulin (E7, NIH Hybridoma Bank, Iowa City, IA). Mouse anti-VSV Matrix was kindly provided by D. Lyles, Wake Forest University. Rabbit anti-ZEBOV-GP1 was kindly provided by A. Sanchez, CDC. Axl-human Fc (Axl amino acids 33–440 attached to human Fc) was purchased from R&D Systems (#154AL).

Pseudotyped particles

Pseudotyped VSV particles—Production of vesicular stomatitis virus (VSV) particles that were pseudotyped with either ZEBOV-GP ΔO or VSV-G was performed as previously described (Takada et al., 1997). Briefly, 293T cells were seeded into 15 cm dishes. The following day 75 μg of the glycoprotein expression plasmid were transfected into the cells

using calcium phosphate transfection as previously described (Brindley et al., 2007). Twenty-four hours following transfection, the cells were washed twice in PBS and transfected 293Ts were transduced with pseudotyped VSV/EGFP/ΔG that expresses EGFP in place of the G glycoprotein at an MOI of 5. Six hours after transduction, the virus inoculum was removed and cells were again washed with PBS. Cell supernatants were collected at 24, 36, and 48 hours following transduction. Stocks were filtered, aliquoted, and stored at −80°C until use.

FIV pseudotyped particles—Pseudotyped FIV viral particles were produced as previously described (Brindley et al., 2007; Sinn et al., 2003). 293T cells were transfected with a total of 75 μg of DNA consisting of plasmids expressing one of three glycoproteins (full length ZEBOV-GP, ZEBOV-GP ΔO or VSV-G), a FIV gag-pol expressing construct (pFIVΔΔ), and a packageable FIV genome that expresses β-galactosidase (pFIVψβgal) at a ratio of 1:2:3 respectively. The DNA was transfected into 15 cm dishes of 293T cells using calcium phosphate transfection. Supernatants were collected at 24, 36, 48, 60 and 72 hours following transfection. The supernatants were filtered through a 0.45 μ filter and pelleted by an overnight centrifugation step (7000 rpm 4°C in a Beckman JA-10 rotor). The viral pellet was resuspended DMEM for an approximate 200 fold concentration. The virus was either used immediately for transduction or stored at −80°C until use.

ZEBOV VLPs—Src-β-lactamase labeled mucin domain deleted ZEBOV virus like particles (ZEBOV ΔO-VLPs) were produced by transfecting 293T cells grown in 15 cm dishes with 75 μg of total DNA at a ratio of 1:2:3:3 for plasmids expressing ZEBOV-NP, ZEBOV-VP40, pZEBOV-GP ΔO and src-β-lactamase fusion protein (Quinn et al., 2009a). pNP and pVP40 were kind gifts from Dr. Ronald Harty (University of Pennsylvania). Supernatants were collected at 24, 36, 48, 60 and 72 hours following transfection. The supernatants were filtered through a 0.45 μ filter and pelleted by an overnight centrifugation step (7000 rpm 4°C in a Beckman JA-10 rotor). The viral pellet was resuspended in DMEM for an approximate 200 fold concentration. The virus was stored at −80°C until use.

NCI 60 screen

4×10^4 cells of 52 cell lines used from the NCI 60 panel (http://dtp.nci.nih.gov/docs/misc/common_files/cell_list.html) were plated in 48-well plates. Relative transduction efficiency was measured using VSV/EGFP/ΔG particles pseudotyped with either VSV-G or ZEBOV-GP ΔO. Twenty hours following transduction the cells were evaluated for EGFP expression by flow cytometry to obtain the transduction efficiency for each cell line. The average of a total of six transduction trials was used as the seed file for COMPARE analysis against the GC235133 gene array data set that used the Affymetrix U133A chip (dtp.nci.nih.gov/docs/misc/common_files/cell_list.html).

Flow cytometry

EGFP expression—Twenty hours following transduction, cells were lifted in 150 μL of Accumax (Fisher Scientific) and analyzed with a FACScan flow cytometer for FL-1 intensity.

Axl staining—Cells were lifted with PBS and 5 mM EDTA and washed 3 times in PBS/5% FCS. Cells were incubated with goat anti-Axl (4 μg/mL) or normal goat sera for 1 hour on ice. Cells were washed and incubated with Cy5-conjugated donkey anti-goat (1:50) (Jackson Immunoresearch) for 30 minutes on ice. Cells were washed and analyzed a with FACScan flow cytometer for FL-4 intensity.

Competition assays

Antibody competition—4×10^4 cells were plated in 48-well plates. The cells were incubated with polyclonal goat antisera (8 μg/mL) against the Axl ectodomain or normal goat serum at 4°C for 30 minutes. Pseudotyped VSV/eGFP/ΔG particles (MOI =0.5) were added to the cells and the plate was shifted to 37°C to promote transduction. Twenty hours following transduction, the cells were lifted in Accumax (Fisher Scientific) and analyzed for eGFP expression using flow cytometry. The percentage of eGFP positive cells was compared to control cells transduced without antisera added.

Axl-Fc competition—VSV/EGFP/ΔG particles pseudotyped with either ZEBOV-GP ΔO or VSV-G were incubated with chimeric Axl ectodomain-Fc protein (Axl-Fc) (R&D Systems) (50 μg/mL) for 30 minutes at 4°C. The mixture was transduced on to SNB-19 or 293T cells in a 48-well plate. Twenty-four hours following transduction, cells were analyzed for EGFP expression using flow cytometry.

Generation of infectious, recombinant ZEBOV-GP ΔO VSV

A molecular clone of VSV containing EGFP in place of G that was generated by Dr. Jack Rose (Haglund et al., 2000) was kindly provided by Dr. Ira Bergman (University of Pittsburgh). The EGFP gene was inserted in place of VSV-G (Gao et al., 2006) and ZEBOV-GP ΔO was inserted upstream from EGFP. The construct along with plasmids expressing VSV N, P, M and L was transfected into BHK 21 cells as previously described (Haglund et al., 2000; Lawson et al., 1995). The full length genome and each of the cDNAs were expressed from a T7 promoter sequence by infection of the cells with vTF7-3, a recombinant vaccinia virus expressing the T7 RNA polymerase. Supernatant was collected, filtered through a 0.2 μ filter and the virus was plaque purified. Immunoblotting of virus stocks verified expression of ZEBOV-GP. Stocks were titered by end point dilution on Vero cells.

Immunoblotting

Axl was detected using a goat polyclonal anti-Axl sera (0.2 μg/mL). Blots were washed and incubated with corresponding secondary HRP-conjugated sera.

Axl RNAi transfections

Two validated *AXL* RNAi constructs were purchased from Invitrogen along with an irrelevant control (Block-It). SNB-19 cells were transfected with 200 pmoles of the RNAi using Lipofectamine 2000. Twenty-four hours following transfection, the cells were lifted with trypsin and distributed into 48-well plates. For all RNAi knock down experiments, cells were examined for Axl protein expression by immunoblotting and for Axl surface expression by flow cytometry at 48 hours. We routinely observed a greater than 90% loss of Axl surface expression and a similar reduction in total Axl expression in cell lysates. In parallel, transfected cells that had been verified for Axl knock down were transduced with FIV particles bearing ZEBOV-GP ΔO FIV/β-galactosidase or VSV-G FIV/ β-galactosidase and assayed for transduction as described above.

Transfection of cells with Axl expression plasmid

An expression plasmid bearing Axl was obtained from the Gene Transfer and Vector Core at the University of Iowa. NCI-H460 and NCI-H522 cells were transfected with 4μg of the Axl expression plasmid or an equivalent empty plasmid using Lipofectamine 2000. Twenty-four hours following transfection, the cells were lifted with trypsin and distributed into 48-well plates. Cells were examined for Axl surface expression by flow cytometry at 48 hours. In parallel, transfected cells were transduced with ZEBOV-GP ΔO or VSV-G VSV

pseudovirions and assayed for transduction by flow cytometry for EGFP expression as described above.

Virus internalization assay

SNB-19 cells seeded in a 6-well plate at a concentration of 5×10^5 cells per well were transfected with 200 pmoles of *AXL* RNAi (described above) or an irrelevant control RNAi (Block-It, Invitrogen) using Lipofectamine 2000. Twenty four hours after transfection, cells were lifted and replated in a 96-well plate at a concentration of 4×10^4 cells per well. The following day, 20 μL of media (containing 10% FBS, 1% P/S and ZEBOV-GP ΔO FIV or VSV-G FIV) were incubated with each well of cells for 1 hour at 4ºC. After 1 hour, media was removed and cells were washed once with 100μL sterile 1X PBS and 100μL of pre-warmed media was added to each well for one hour at 37°C. At the termination of the experiment, media was removed. Cells were lifted and extracellular virus removed with a five minute incubation with 100 μL of 0.25% trypsin/5 mM EDTA treatment. Trypsin/EDTA was neutralized with DMEM with FCS, and the cells were pelleted in a microcentrifuge for 4 minutes at 14,000 rpm. Supernatants were removed, and the pellet was lysed in 25μL of sterile 1X PBS containing 1% SDS. As a control, after the 4ºC incubation, cells were washed once and then lysed to determine the 100% value for total bound virions after one hour. Cell lysates were kept at −20º C until analysis by immunoblotting for β-actin or FIV capsid.

Immunoblot analysis of viral internalization assay

Proteins present in the cell lysates were separated on a 4–12% Bis-Tris NuPAGE gel (Invitrogen) and transferred onto nitrocellulose. FIV Capsid was detected by incubating with polyclonal anti-FIV antibody (1:5000; obtained locally from FIV seropositive cats) overnight at 4ºC and with secondary peroxidase-conjugated goat anti-feline antiserum (1:20,000; Amersham). β-actin was detected by incubating with a monoclonal anti-β-actin antibody conjugated to peroxidase (1:10,000; Abcam) for 2 hours at room temperature. Membranes were visualized using a Fujifilm Image Reader LAS-3000 (Fujifilm, Stamford, CT) and using the chemiluminescence method according to the manufacturer's protocol (Pierce). Data was analyzed and quantified using the Fujifilm Multi Gauge V2.3 program (Fujifilm, Stamford, CT). Data are presented as the ratio of FIV Capsid to β-actin for each sample divided by the control ratio times 100%.

Viral transduction of *AXL* RNAi transfected cells with thermolysin-treated virus

SNB-19 cells were transfected with *AXL* RNAi as described above. 24 hours after transfection, cells were plated in a 48-well format at a concentration of 3.5×10^4 cells per well. FIV/β-gal pseudovirions bearing full length ZEBOV-GP were treated for 5 minutes at 37ºC with 0.1 mg/mL of thermolysin (Sigma-Aldrich). Virus was then treated with 5mM EDTA or 5 minutes at room temperature to neutralize the thermolysin. Thermolysin-treated or mock-treated virus was added to transfected cells at 48 hours following transfection. Six hours after the addition of thermolysin treated virus, the virus was removed, media refreshed, and cells incubated for an additional 48 hours at 37ºC. At the termination of the experiment, cells were fixed in PBS with 3.7% formalin and evaluated for β-gal activity using the substrate 5-bromo-4-chloro-3-indolyl-β-D-galactopyranoside. The number of β-gal-positive cells was enumerated by microscopic visual inspection. The findings are shown as the ratio of the number of transduced cells found in each treatment divided by control values.

Membrane fusion assay

SNB-19 cells were seeded at 3×10^4 cells per well of 96 well and incubated with 20 μg/mL (1:20) of goat anti-Axl antisera or normal goat sera for 1 hour at 4ºC. Cells were shifted to 37ºC and incubated with 50μL of Src-β-lactamase containing ZEBOV-GP ΔO VLPs per well. After 12 h, VLPs within the media were removed and 0.1 mM CCF2-AM substrate was added to each well diluted in 100 μL DMEM according to manufacturer's protocol (Invitrogen). Positive controls for the lactamase assay included pCMV-src-β-lactamase transfected and blue fluorescent protein (BFP) transfected cells. The plate was covered and incubated at room temperature for 2 hours away from direct sunlight. After 2 hours, the cells were trypsinized with 0.05% trypsin-EDTA (50 μL per well) and resuspended in a total volume of 100 μL (50 μL trypsin + 50 μL DMEM). Blue/green fluorescence was quantified in the cells using a three laser FACS Aria (Becton Dickinson) equipped with a 407 violet, a 488 blue, and a 633 red laser. Blue and green fluorescence was measured separately with emission filters 450/40 nm and 530/30 nm, respectively. The background blue fluorescence of untreated, CCF2-AM loaded control cells was subtracted as autofluorescence. Blue fluorescence was expressed as percentage blue cells in the population.

Confocal microscopy

SNB-19 cells (3.5×10^4 cells) were plated on collagen-coated coverslips and incubated overnight at 37°C to allow cell adherence. Cells were incubated with ZEBOV-GP ΔO or VSV-G FIV pseudovirions (MOI=250) at 4°C for 1 hour. Unbound virus was removed, cells were washed once in 1X PBS, and cells were shifted to 37°C in pre-warmed media for the indicated times. At the indicated time, cells were fixed in 2% paraformaldehyde and not permeabilized or permeabilized with 0.2% Triton X-100. Virus (green) was detected with anti-FIV monoclonal antibody (1:50; NIAID AIDS Research and Reference Reagent Program) and Alexa Fluor 488 chicken α-mouse (1:200; Invitrogen). Axl (red) was detected with anti-human Axl polyclonal antibody (1:150; R&D Systems) and Alexa Fluor 568 donkey α-goat (1:200; Invitrogen). Microscopy was performed on a Nikon 801 confocal microscope with the gain set at the beginning of data collection and not subsequently changed.

Statistical analysis

Studies were performed at least three independent times except where noted in the figure legends. Means and standard errors of the mean are shown. Student's t-test was used to generate a p value to evaluate the statistical differences between treatments, utilizing the two-tailed distribution and two sample equal-variance conditions. Significance of the correlation findings in the NCI 60 screen was assessed by performing a linear correlation and regression and determining the p value from the two tailed distribution. A significant difference was determined by a p-value of < 0.05 and level of significance was noted in each figure. If the p-value was > 0.05, the data were not considered statistically significantly different.

Supplementary Material

Refer to Web version on PubMed Central for supplementary material.

Acknowledgments

This work was supported by NIH AI064526 and AI073330 (W.M.), NIH HL075363 (P.B.M.) and intramural NIH NIAID biodefense and NIH NIDCR grants to J.A.C. M.A.B. and A.S.K. were supported through NIH T32 A1007533 a training grant in molecular virology.

References

Allavena P, Chieppa M, Monti P, Piemonti L. From pattern recognition receptor to regulator of homeostasis: the double-faced macrophage mannose receptor. Crit Rev Immunol. 2004; 24:179–192. [PubMed: 15482253]

Alvarez CP, Lasala F, Carrillo J, Muniz O, Corbi AL, Delgado R. C-type lectins DC-SIGN and L-SIGN mediate cellular entry by Ebola virus in cis and in trans. J Virol. 2002; 76:6841–6844. [PubMed: 12050398]

Baribaud F, Doms RW, Pohlmann S. The role of DC-SIGN and DC-SIGNR in HIV and Ebola virus infection: can potential therapeutics block virus transmission and dissemination? Expert Opin Ther Targets. 2002; 6:423–431. [PubMed: 12223058]

Bhattacharyya S, Warfield KL, Ruthel G, Bavari S, Aman MJ, Hope TJ. Ebola virus uses clathrin-mediated endocytosis as an entry pathway. Virology. 2010; 401:18–28. [PubMed: 20202662]

Braunger J, Schleithoff L, Schulz AS, Kessler H, Lammers R, Ullrich A, Bartram CR, Janssen JW. Intracellular signaling of the Ufo/Axl receptor tyrosine kinase is mediated mainly by a multi-substrate docking-site. Oncogene. 1997; 14:2619–2631. [PubMed: 9178760]

Brindley MA, Hughes L, Ruiz A, McCray PB Jr, Sanchez A, Sanders DA, Maury W. Ebola virus glycoprotein 1: identification of residues important for binding and postbinding events. J Virol. 2007; 81:7702–7709. [PubMed: 17475648]

Budagian V, Bulanova E, Orinska Z, Thon L, Mamat U, Bellosta P, Basilico C, Adam D, Paus R, Bulfone-Paus S. A promiscuous liaison between IL-15 receptor and Axl receptor tyrosine kinase in cell death control. Embo J. 2005; 24:4260–4270. [PubMed: 16308569]

Caberoy NB, Zhou Y, Li W. Tubby and tubby-like protein 1 are new MerTK ligands for phagocytosis. The EMBO journal. 2010; 29:3898–3910. [PubMed: 20978472]

Carroll K, Gomez C, Shapiro L. Tubby proteins: the plot thickens. Nat Rev Mol Cell Biol. 2004; 5:55–63. [PubMed: 14708010]

Cavrois M, De Noronha C, Greene WC. A sensitive and specific enzyme-based assay detecting HIV-1 virion fusion in primary T lymphocytes. Nat Biotechnol. 2002; 20:1151–1154. [PubMed: 12355096]

Cavrois M, Neidleman J, Bigos M, Greene WC. Fluorescence resonance energy transfer-based HIV-1 virion fusion assay. Methods Mol Biol. 2004; 263:333–344. [PubMed: 14976375]

Chan SY, Empig CJ, Welte FJ, Speck RF, Schmaljohn A, Kreisberg JF, Goldsmith MA. Folate receptor-alpha is a cofactor for cellular entry by Marburg and Ebola viruses. Cell. 2001; 106:117–126. [PubMed: 11461707]

Chandran K, Sullivan NJ, Felbor U, Whelan SP, Cunningham JM. Endosomal proteolysis of the Ebola virus glycoprotein is necessary for infection. Science. 2005; 308:1643–1645. [PubMed: 15831716]

Demarchi F, Verardo R, Varnum B, Brancolini C, Schneider C. Gas6 anti-apoptotic signaling requires NF-kappa B activation. J Biol Chem. 2001; 276:31738–31744. [PubMed: 11425860]

Di Pasquale G, Davidson BL, Stein CS, Martins I, Scudiero D, Monks A, Chiorini JA. Identification of PDGFR as a receptor for AAV-5 transduction. Nat Med. 2003; 9:1306–1312. [PubMed: 14502277]

Fridell YW, Villa J Jr, Attar EC, Liu ET. GAS6 induces Axl-mediated chemotaxis of vascular smooth muscle cells. J Biol Chem. 1998; 273:7123–7126. [PubMed: 9507025]

Gao Y, Whitaker-Dowling P, Watkins SC, Griffin JA, Bergman I. Rapid adaptation of a recombinant vesicular stomatitis virus to a targeted cell line. J Virol. 2006; 80:8603–8612. [PubMed: 16912309]

Geijtenbeek TB, Gringhuis SI. Signalling through C-type lectin receptors: shaping immune responses. Nat Rev Immunol. 2009; 9:465–479. [PubMed: 19521399]

Geijtenbeek TB, van Kooyk Y. Pathogens target DC-SIGN to influence their fate DC-SIGN functions as a pathogen receptor with broad specificity. APMIS. 2003; 111:698–714. [PubMed: 12974773]

Goruppi S, Chiaruttini C, Ruaro ME, Varnum B, Schneider C. Gas6 induces growth, beta-catenin stabilization, and T-cell factor transcriptional activation in contact-inhibited C57 mammary cells. Mol Cell Biol. 2001; 21:902–915. [PubMed: 11154277]

Goruppi S, Ruaro E, Varnum B, Schneider C. Requirement of phosphatidylinositol 3-kinase-dependent pathway and Src for Gas6-Axl mitogenic and survival activities in NIH 3T3 fibroblasts. Mol Cell Biol. 1997; 17:4442–4453. [PubMed: 9234702]

Goruppi S, Ruaro E, Varnum B, Schneider C. Gas6-mediated survival in NIH3T3 cells activates stress signalling cascade and is independent of Ras. Oncogene. 1999; 18:4224–4236. [PubMed: 10435635]

Hafizi S, Gustafsson A, Stenhoff J, Dahlback B. The Ran binding protein RanBPM interacts with Axl and Sky receptor tyrosine kinases. Int J Biochem Cell Biol. 2005; 37:2344–2356. [PubMed: 15964779]

Haglund K, Forman J, Krausslich HG, Rose JK. Expression of human immunodeficiency virus type 1 Gag protein precursor and envelope proteins from a vesicular stomatitis virus recombinant: high-level production of virus-like particles containing HIV envelope. Virology. 2000; 268:112–121. [PubMed: 10683333]

Heiring C, Dahlback B, Muller YA. Ligand recognition and homophilic interactions in Tyro3: structural insights into the Axl/Tyro3 receptor tyrosine kinase family. J Biol Chem. 2004; 279:6952–6958. [PubMed: 14623883]

Hunt CL, Kolokoltsov AA, Davey RA, Maury W. The Tyro3 receptor kinase Axl enhances macropinocytosis of Zaire ebolavirus. J Virol. 2011; 85:334–347. [PubMed: 21047970]

Jeffers SA, Sanders DA, Sanchez A. Covalent modifications of the ebola virus glycoprotein. J Virol. 2002; 76:12463–12472. [PubMed: 12438572]

Kerrigan AM, Brown GD. Syk-coupled C-type lectin receptors that mediate cellular activation via single tyrosine based activation motifs. Immunol Rev. 2010; 234:335–352. [PubMed: 20193029]

Lasala F, Arce E, Otero JR, Rojo J, Delgado R. Mannosyl glycodendritic structure inhibits DC-SIGN-mediated Ebola virus infection in cis and in trans. Antimicrob Agents Chemother. 2003; 47:3970–3972. [PubMed: 14638512]

Lawson ND, Stillman EA, Whitt MA, Rose JK. Recombinant vesicular stomatitis viruses from DNA. Proc Natl Acad Sci U S A. 1995; 92:4477–4481. [PubMed: 7753828]

Lee WP, Liao Y, Robinson D, Kung HJ, Liu ET, Hung MC. Axl-gas6 interaction counteracts E1A-mediated cell growth suppression and proapoptotic activity. Mol Cell Biol. 1999; 19:8075–8082. [PubMed: 10567533]

Lin G, Simmons G, Pohlmann S, Baribaud F, Ni H, Leslie GJ, Haggarty BS, Bates P, Weissman D, Hoxie JA, Doms RW. Differential N-linked glycosylation of human immunodeficiency virus and Ebola virus envelope glycoproteins modulates interactions with DC-SIGN and DC-SIGNR. J Virol. 2003; 77:1337–1346. [PubMed: 12502850]

Linger RM, Keating AK, Earp HS, Graham DK. TAM receptor tyrosine kinases: biologic functions, signaling, and potential therapeutic targeting in human cancer. Adv Cancer Res. 2008; 100:35–83. [PubMed: 18620092]

Marzi A, Gramberg T, Simmons G, Moller P, Rennekamp AJ, Krumbiegel M, Geier M, Eisemann J, Turza N, Saunier B, Steinkasserer A, Becker S, Bates P, Hofmann H, Pohlmann S. DC-SIGN and DC-SIGNR interact with the glycoprotein of Marburg virus and the S protein of severe acute respiratory syndrome coronavirus. J Virol. 2004; 78:12090–12095. [PubMed: 15479853]

McCloskey P, Fridell YW, Attar E, Villa J, Jin Y, Varnum B, Liu ET. GAS6 mediates adhesion of cells expressing the receptor tyrosine kinase Axl. J Biol Chem. 1997; 272:23285–23291. [PubMed: 9287338]

Melaragno MG, Cavet ME, Yan C, Tai LK, Jin ZG, Haendeler J, Berk BC. Gas6 inhibits apoptosis in vascular smooth muscle: role of Axl kinase and Akt. J Mol Cell Cardiol. 2004; 37:881–887. [PubMed: 15380678]

Nielsen-Preiss SM, Allen MP, Xu M, Linseman DA, Pawlowski JE, Bouchard RJ, Varnum BC, Heidenreich KA, Wierman ME. Adhesion-related kinase induction of migration requires phosphatidylinositol-3-kinase and ras stimulation of rac activity in immortalized gonadotropin-releasing hormone neuronal cells. Endocrinology. 2007; 148:2806–2814. [PubMed: 17332061]

Quinn K, Brindley MA, Weller ML, Kaludov N, Kondratowicz A, Hunt CL, Sinn PL, McCray PB Jr, Stein CS, Davidson BL, Flick R, Mandell R, Stapleton W, Maury W, Chiorini JA. Rho GTPases Modulate Entry of Ebola and Vesicular Stomatitis Pseudotyped Vectors. J Virol. 2009a

Quinn K, Brindley MA, Weller ML, Kaludov N, Kondratowicz A, Hunt CL, Sinn PL, McCray PB Jr, Stein CS, Davidson BL, Flick R, Mandell R, Staplin W, Maury W, Chiorini JA. Rho GTPases modulate entry of Ebola virus and vesicular stomatitis virus pseudotyped vectors. J Virol. 2009b; 83:10176–10186. [PubMed: 19625394]

Quinn K, Brindley MA, Weller ML, Kaludov N, Kondratowicz A, Hunt CL, Sinn PL, McCray PB Jr, Stein CS, Davidson DL, Flick R, Mandell R, Stapleton W, Maury W, Chiorini JA. Rho GTPases Modulate Entry of Ebola and Vesicular Stomatitis Pseudotyped Vectors submitted. 2009

Sasaki T, Knyazev PG, Clout NJ, Cheburkin Y, Gohring W, Ullrich A, Timpl R, Hohenester E. Structural basis for Gas6-Axl signalling. EMBO J. 2006; 25:80–87. [PubMed: 16362042]

Schornberg K, Matsuyama S, Kabsch K, Delos S, Bouton A, White J. Role of endosomal cathepsins in entry mediated by the Ebola virus glycoprotein. J Virol. 2006; 80:4174–4178. [PubMed: 16571833]

Scott RS, McMahon EJ, Pop SM, Reap EA, Caricchio R, Cohen PL, Earp HS, Matsushima GK. Phagocytosis and clearance of apoptotic cells is mediated by MER. Nature. 2001; 411:207–211. [PubMed: 11346799]

Shao WH, Zhen Y, Eisenberg RA, Cohen PL. The Mer receptor tyrosine kinase is expressed on discrete macrophage subpopulations and mainly uses Gas6 as its ligand for uptake of apoptotic cells. Clin Immunol. 2009; 133:138–144. [PubMed: 19631584]

Shimojima M, Ikeda Y, Kawaoka Y. The mechanism of Axl-mediated Ebola virus infection. J Infect Dis. 2007; 196(Suppl 2):S259–263. [PubMed: 17940958]

Shimojima M, Takada A, Ebihara H, Neumann G, Fujioka K, Irimura T, Jones S, Feldmann H, Kawaoka Y. Tyro3 family-mediated cell entry of Ebola and Marburg viruses. J Virol. 2006; 80:10109–10116. [PubMed: 17005688]

Simmons G, Reeves JD, Grogan CC, Vandenberghe LH, Baribaud F, Whitbeck JC, Burke E, Buchmeier MJ, Soilleux EJ, Riley JL, Doms RW, Bates P, Pohlmann S. DC-SIGN and DC-SIGNR bind ebola glycoproteins and enhance infection of macrophages and endothelial cells. Virology. 2003a; 305:115–123. [PubMed: 12504546]

Simmons G, Rennekamp AJ, Chai N, Vandenberghe LH, Riley JL, Bates P. Folate receptor alpha and caveolae are not required for Ebola virus glycoprotein-mediated viral infection. J Virol. 2003b; 77:13433–13438. [PubMed: 14645601]

Sinn PL, Hickey MA, Staber PD, Dylla DE, Jeffers SA, Davidson BL, Sanders DA, McCray PB Jr. Lentivirus vectors pseudotyped with filoviral envelope glycoproteins transduce airway epithelia from the apical surface independently of folate receptor alpha. J Virol. 2003; 77:5902–5910. [PubMed: 12719583]

Son BK, Kozaki K, Iijima K, Eto M, Nakano T, Akishita M, Ouchi Y. Gas6/Axl-PI3K/Akt pathway plays a central role in the effect of statins on inorganic phosphate-induced calcification of vascular smooth muscle cells. Eur J Pharmacol. 2007; 556:1–8. [PubMed: 17196959]

Stitt TN, Conn G, Gore M, Lai C, Bruno J, Radziejewski C, Mattsson K, Fisher J, Gies DR, Jones PF, et al. The anticoagulation factor protein S and its relative, Gas6, are ligands for the Tyro 3/Axl family of receptor tyrosine kinases. Cell. 1995; 80:661–670. [PubMed: 7867073]

Takada A, Fujioka K, Tsuiji M, Morikawa A, Higashi N, Ebihara H, Kobasa D, Feldmann H, Irimura T, Kawaoka Y. Human macrophage C-type lectin specific for galactose and N-acetylgalactosamine promotes filovirus entry. J Virol. 2004; 78:2943–2947. [PubMed: 14990712]

Takada A, Robison C, Goto H, Sanchez A, Murti KG, Whitt MA, Kawaoka Y. A system for functional analysis of Ebola virus glycoprotein. Proc Natl Acad Sci U S A. 1997; 94:14764–14769. [PubMed: 9405687]

Varnum BC, Young C, Elliott G, Garcia A, Bartley TD, Fridell YW, Hunt RW, Trail G, Clogston C, Toso RJ, et al. Axl receptor tyrosine kinase stimulated by the vitamin K-dependent protein encoded by growth-arrest-specific gene 6. Nature. 1995; 373:623–626. [PubMed: 7854420]

Weinger JG, Gohari P, Yan Y, Backer JM, Varnum B, Shafit-Zagardo B. In brain, Axl recruits Grb2 and the p85 regulatory subunit of PI3 kinase; in vitro mutagenesis defines the requisite binding sites for downstream Akt activation. J Neurochem. 2008; 106:134–146. [PubMed: 18346204]

Weller ML, Amornphimoltham P, Schmidt M, Wilson PA, Gutkind JS, Chiorini JA. Epidermal growth factor receptor is a co-receptor for adeno-associated virus serotype 6. Nat Med. 2010; 16:662–664. [PubMed: 20473307]

Wilhelm I, Nagyoszi P, Farkas AE, Couraud PO, Romero IA, Weksler B, Fazakas C, Dung NT, Bottka S, Bauer H, Bauer HC, Krizbai IA. Hyperosmotic stress induces Axl activation and cleavage in cerebral endothelial cells. J Neurochem. 2008; 107:116–126. [PubMed: 18673450]

Wool-Lewis RJ, Bates P. Characterization of Ebola virus entry by using pseudotyped viruses: identification of receptor-deficient cell lines. J Virol. 1998; 72:3155–3160. [PubMed: 9525641]

Zhang YX, Knyazev PG, Cheburkin YV, Sharma K, Knyazev YP, Orfi L, Szabadkai I, Daub H, Keri G, Ullrich A. AXL is a potential target for therapeutic intervention in breast cancer progression. Cancer Res. 2008; 68:1905–1915. [PubMed: 18339872]

Zheng Y, Zhang L, Lu Q, Wang X, Yu F, Wang X, Lu Q. NGF-induced Tyro3 and Axl function as survival factors for differentiating PC12 cells. Biochem Biophys Res Commun. 2009; 378:371–375. [PubMed: 19027714]

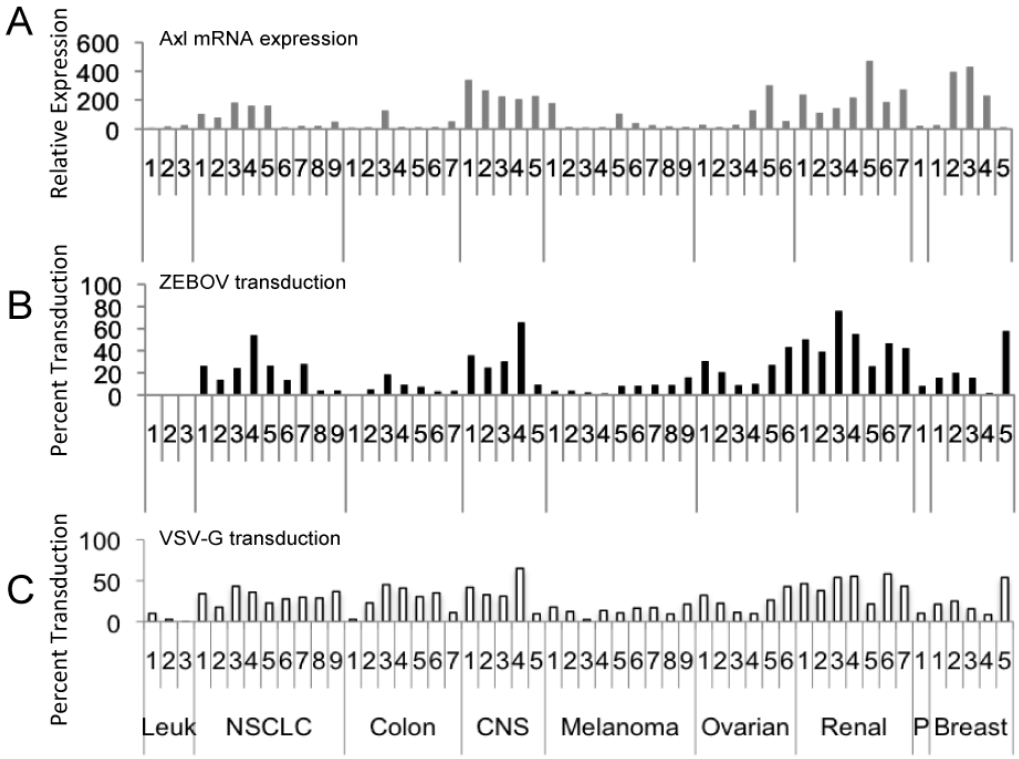

Fig. 1. Correlation of ZEBOV-GP pseudotyped VSV transduction with *AXL* expression in the NCI-60 panel of human tumor cells

A) Relative expression of *AXL* mRNA expression in the 52 cell lines analyzed in the screen. **B)** ZEBOV-GP ΔO VSV transduction of the 52 lines. **C)** VSV-G VSV transduction of the same lines. *AXL* expression and ZEBOV-GP ΔO-dependent transduction, but not VSV-G-dependent transduction were positively correlated in our transduction screen with a Pearson correlation coefficient (PCC) of 0.517 ($p<0.0001$). Data shown are the mean of three independent sets of transductions. Gene array data from the individual arrays are available at http://dtp.nci.nih.gov/mtargets/download.html. The data set compared in this study was GC11900. Leuk = leukemia lines; NSCLC = non-small cell lung carcinoma; CNS = central nervous system; P = prostate.

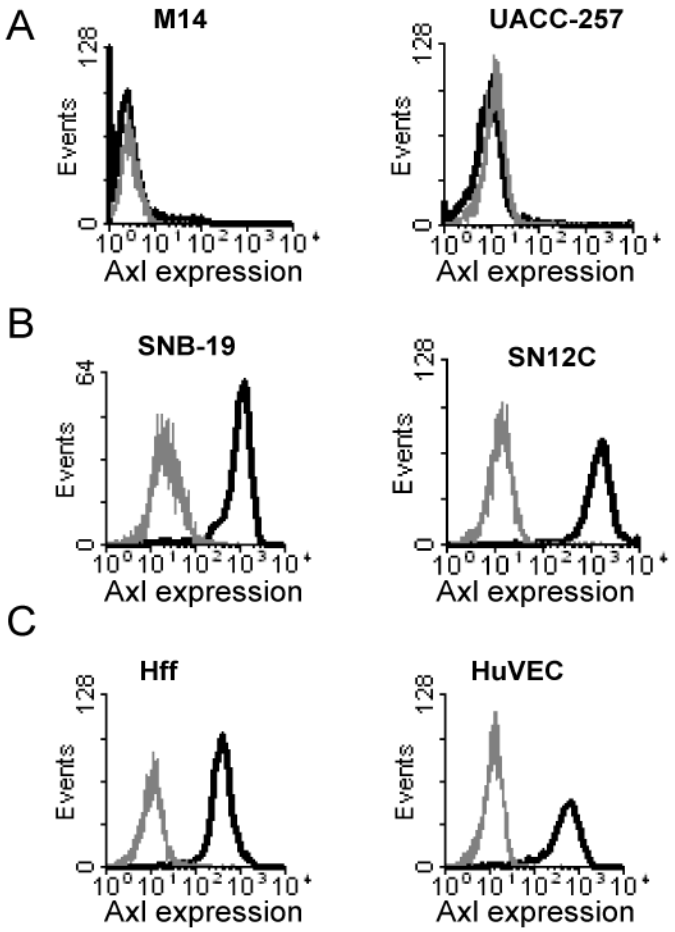

Fig. 2. Cell surface Axl expression

A) Axl surface expression on two NCI-60 cell lines that were poorly transduced with ZEBOV-GP ΔO VSV and displayed low levels of *AXL* expression in NCI-60 gene array studies. **B)** Axl surface expression on two NCI-60 cell lines that were highly transduced with ZEBOV-GP ΔO VSV and displayed robust levels of *AXL* mRNA expression on the gene arrays. **C)** Axl expression on the surface of two primary human cell populations, human foreskin fibroblasts (Hff) and umbilical cord endothelial cells (HuVEC). Cells stained with normal goat sera are shown in grey histograms, whereas cells stained with goat anti-human Axl antisera are shown in black histograms.

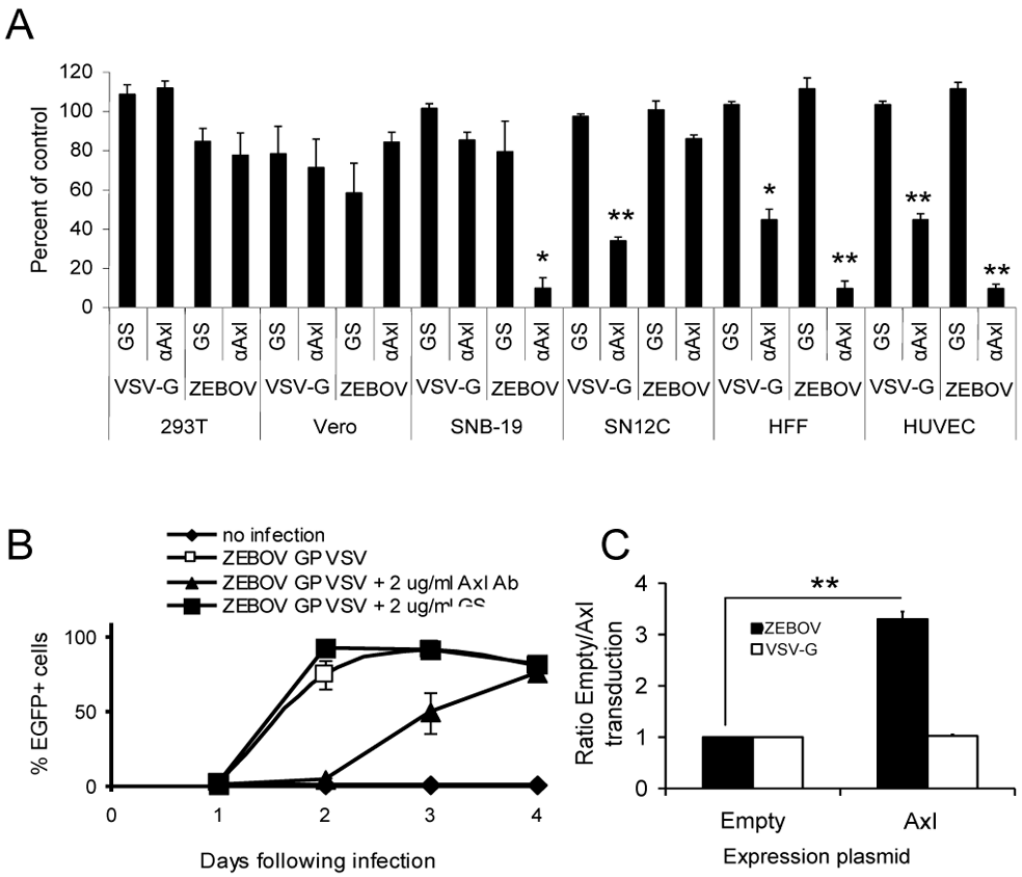

Fig. 3. The impact of Axl on ZEBOV transduction is cell dependent

A) Ability of Axl antisera to block ZEBOV-GP- and VSV G-dependent transduction. Cells were incubated with 8 μg/mL of goat anti-Axl sera or normal goat serum (GS) at 4ºC for 30 minutes. VSV-G or ZEBOV-GP ΔO pseudotyped VSV (MOI =0.5) was added to cells and shifted to 37ºC. Twenty hours following transduction, the cells were analyzed for EGFP expression using flow cytometry. Relative transduction values in the presence of antisera are shown as the percent of transduction in the absence of antisera (control values) for each cell population. Shown are the mean and standard error of the mean of three independent experiments. *, $p < 0.05$; **, $p < 0.001$. **B)** Ability of Axl antisera to reduce infection of recombinant ZEBOV-GP ΔO VSV. SNB-19 cells were pre-incubated with either 2 μg/mL of anti-Axl antisera or normal goat sera (GS) for 15 minutes prior to addition of virus (MOI= 0.1). Cells were assessed for EGFP expression on days noted. Shown are the mean and standard error of the mean of one experiment that is representative of three independent studies that were performed. **C)** Ability of Axl expression to increase ZEBOV-GP ΔO pseudotyped VSV entry in the poorly permissive NCI-H522 cell line. NCI-H522 cells were transfected with empty plasmid or plasmid expressing Axl and transduced with VSV pseudotypes (MOI 0.005) 48 h following transfection. Cells were analyzed for EGFP expression 24 h following transduction by flow cytometry. A ratio of transduction relative to transduction in the presence of empty plasmid are shown. Shown are the mean and standard error of the mean of three independent experiments. **, $p < 0.001$

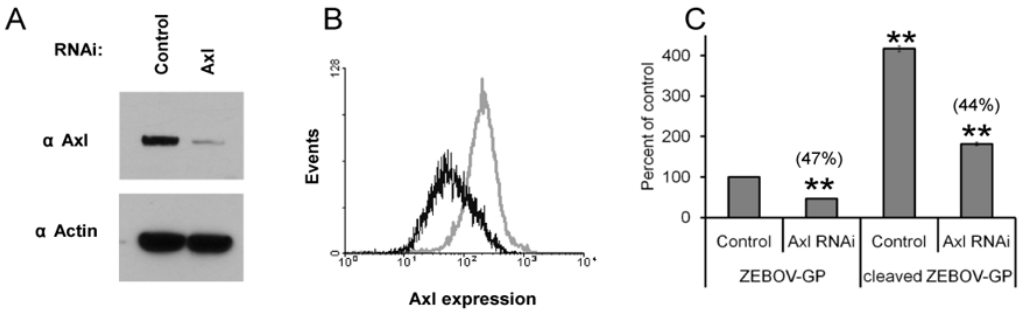

Fig. 4. Thermolysin-treated ZEBOV-GP pseudovirions remain sensitive to *AXL* RNAi treatment

A and B) Knockdown of Axl expression in SNB-19 cells by validated *AXL* siRNA (Invitrogen) at 48 hours following transfection as assessed by immunoblotting of cell lysates for Axl (A) or cell surface expression of Axl (B). Shown in the black histogram are cells treated with *AXL* RNAi; the grey histogram represents cells treated with an irrelevant RNAi. **C)** Thermolysin treated full length ZEBOV-GP FIV pseudovirions remain sensitive to *AXL* RNAi treatment. Virions were treated with thermolysin or mock treated and added to SNB-19 cells that were treated with either *AXL* RNAi or an irrelevant RNAi. Cells were evaluated at 48 hours following transduction for β-gal expression. The findings are shown as the ratio of the number of transduced cells found in each treatment divided by control values. The numbers in parenthesis represent the effect of *AXL* RNAi treatment on transduction relative to the respective control. **, $p < 0.001$.

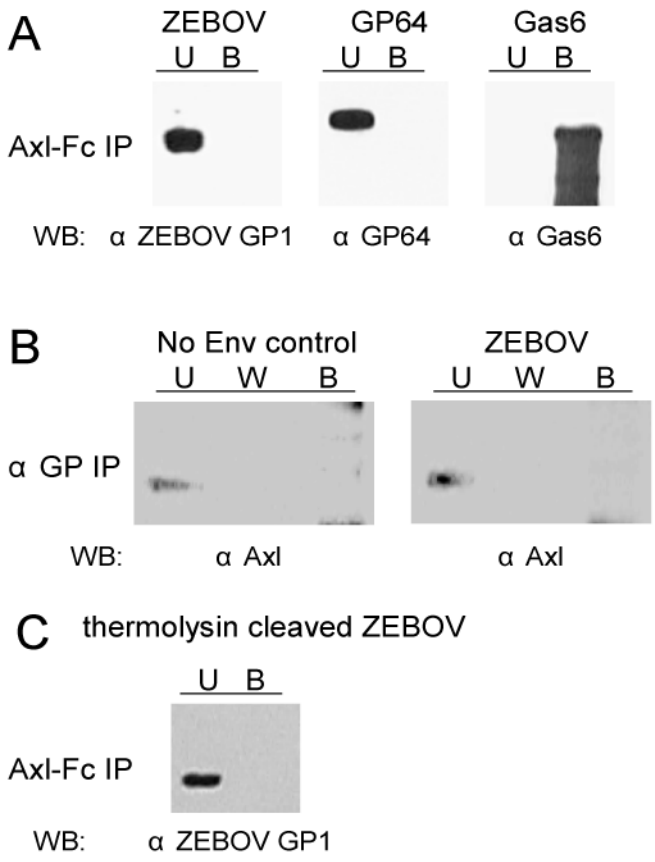

Fig. 5. Direct interactions between ZEBOV-GP and Axl cannot be detected

A) Axl-Fc (0.5 μg) was bound to Protein A sepharose beads and incubated with ZEBOV-GP ΔO or baculovirus GP64 pseudotyped FIV particles. Pull down of Gas6 (0.5 μg) served as a positive control in this study. U, unbound; B, Axl-Fc bound. **B)** ZEBOV pseudotyped particles were bound to protein G beads with anti-ZEBOV-GP1 antisera. SNB-19 cell lysates were passed over the beads and the unbound (U), wash (W), and bound (B) fractions were examined for Axl by immunoblot. **C)** Axl-Fc does not interact with thermolysin-cleaved ZEBOV FIV particles.

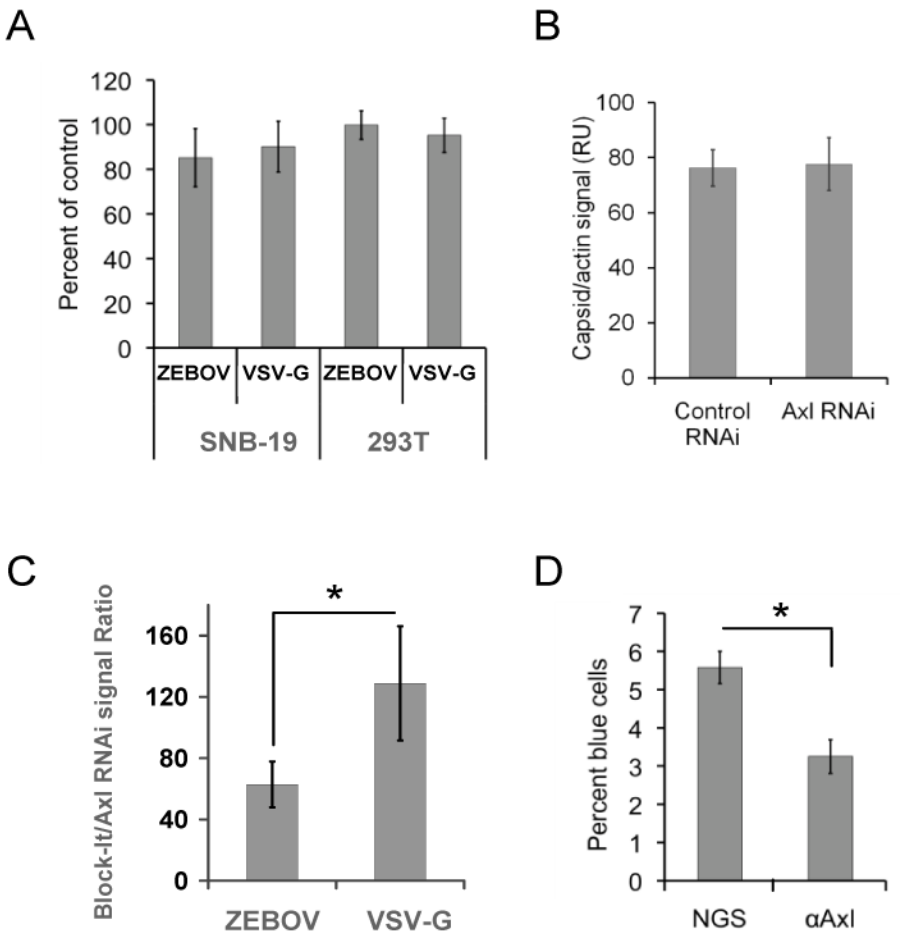

Fig. 6. Axl is required for post-binding events

A) Soluble Axl-Fc does not interfere with ZEBOV-GP ΔO pseudotyped VSV transduction. ZEBOV and VSV-G virions were pre-incubated with Axl-Fc (50 μg/mL) and transduced on to Axl dependent SNB-19 cells or the Axl-independent 293T cells. Transduction was evaluated by EGFP expression in the transduced populations at 24 hours. Results are shown as the number of cells transduced in the presence of Axl-Fc divided by the number of transduced cells in the absence of treatment. **B)** RNAi knock down of Axl had no effect on ZEBOV-GP ΔO pseudovirion binding. Forty-eight hours following transfection of *AXL* RNAi or an irrelevant RNAi into SNB-19 cells, equivalent quantities of ZEBOV-GP ΔO FIV were incubated with cells for one hour at 4°C. Unbound virus was removed and cells were lysed. Lysates were immunoblotted for FIV capsid and quantitated as described in the Materials and Methods. Shown is average pixel values of FIV capsid on the immunoblot divided by the average pixel values for cellular β-actin from 10 independent experiments. **C)** ZEBOV-GP ΔO FIV internalization, but not VSV-G FIV is decreased in *AXL* siRNA-treated cells. SNB-19 cells were transfected with *AXL* siRNA or an irrelevant control siRNA. At 48 hours, ZEBOV-GP ΔO FIV pseudovirions were bound to the cells for 1 hour at 4°C. Unbound virus was removed and cells were shifted to 37°C for 2 hour. Cells were lysed and immunoblotted for FIV capsid and cellular actin. The capsid signal was normalized for actin levels and data are reported as the ratio of the FIV signal in the Axl knock down cells divided by the FIV signal in the cells transfected with an irrelevant RNA. **D)** Ability of Axl antisera to block ZEBOV VLP fusion events. ZEBOV-GP ΔO-VLPs containing Src-β-lactamase were transduced into SNB-19 cells in the presence or absence of 1:20 dilution of

polyclonal antisera against the ectodomain of Axl or normal goat sera (NGS). Entry of β-lactamase into the cytoplasm of cells was evaluated by flow cytometry following incubation of the cells with the fluorescent β-lactamase substrate CCF2/AM for 2 hours. *$p < 0.05$.

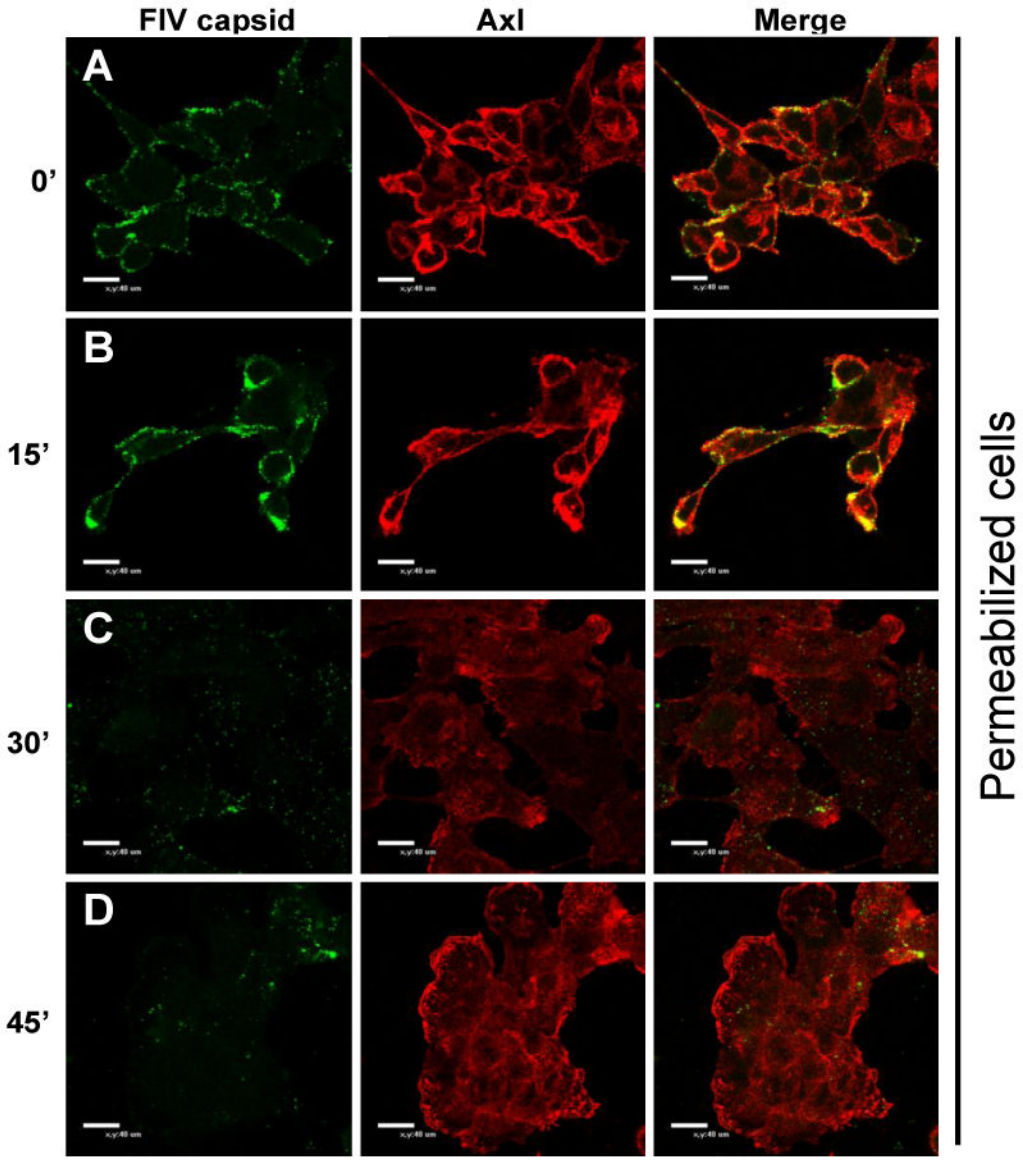

Fig. 7. Axl transiently associated with ZEBOV-GP ΔO pseudovirions on the cell surface and is internalized as virions enter cells

Confocal microscopy of Axl and FIV capsid during ZEBOV-GP ΔO FIV transduction. **A)** Localization of Axl and FIV capsid expression in SNB-19 cells incubated with ZEBOV-GP ΔO FIV (MOI=250) for 1 hour at 4°C. **B–D)** Localization of Axl and FIV capsid in SNB-19 cells following incubation of ZEBOV-GP ΔO FIV (MOI=250) for 1 hour at 4°C, removal of unbound virions and incubation of cells with pre-warmed media at 37°C for 15 minutes (B), 30 minutes (C) or 45 minutes (D). All coverslips were fixed with 2% paraformaldehyde, permeabilized with 0.2% Triton X-100 and immunostained with goat anti-Axl and mouse anti-FIV capsid. Findings shown in panels are representative experiments performed three independent times.

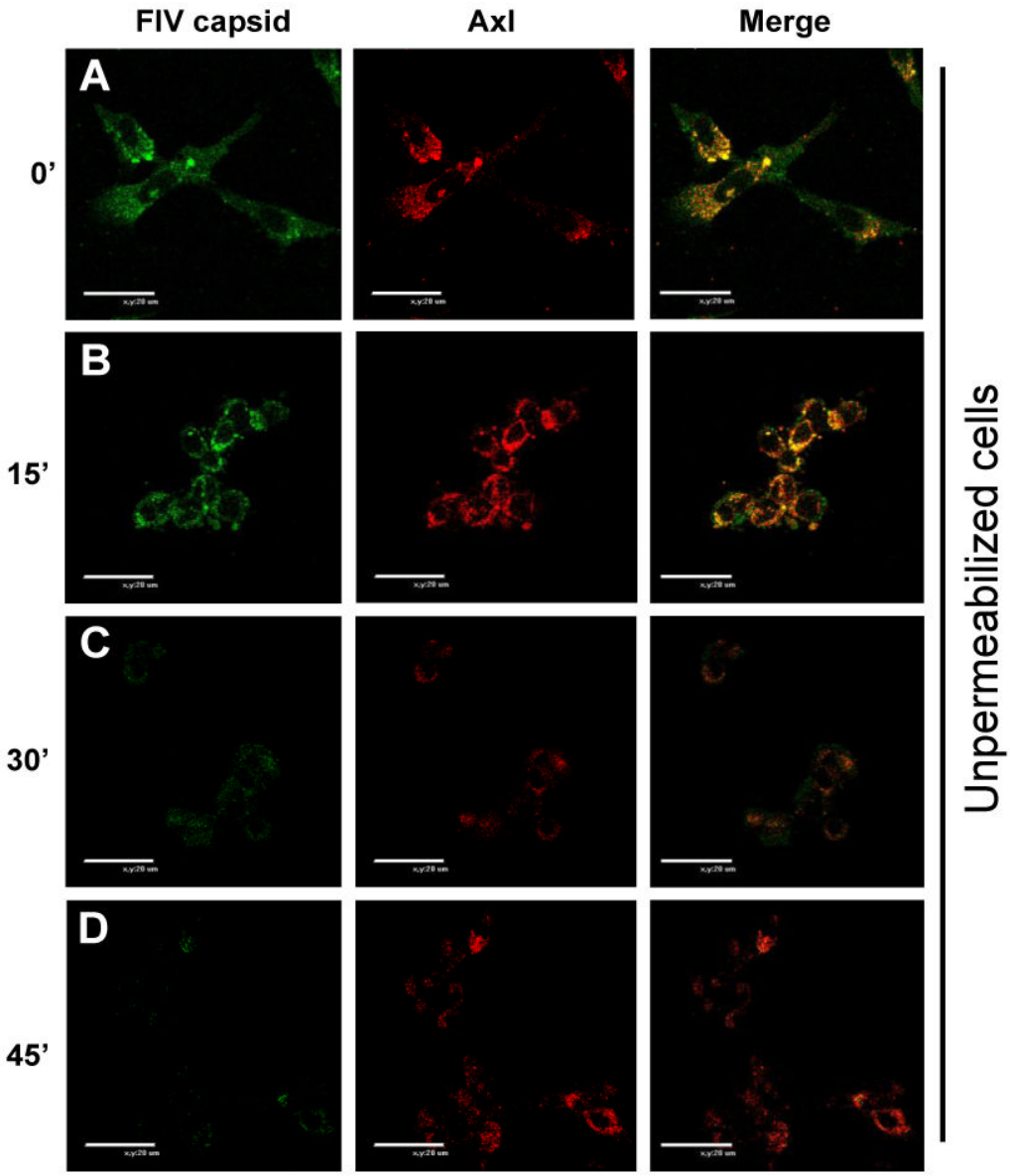

Fig. 8. Both Axl and ZEBOV-GP ΔO pseudovirions are internalized from the cell surface during infection

Confocal microscopy of Axl and FIV capsid during ZEBOV-GP ΔO FIV transduction in non-permeabilized cells. **A)** Localization of Axl and FIV capsid expression in SNB-19 cells incubated with ZEBOV-GP ΔO FIV (MOI=250) for 1 hour at 4°C. **B–D)** Localization of Axl and FIV capsid in SNB-19 cells following incubation of ZEBOV-GP ΔO FIV (MOI=250) for 1 hour at 4°C, removal of unbound virions and incubation of cells with pre-warmed media at 37°C for 15 minutes (B), 30 minutes (C) or 45 minutes (D). All coverslips were fixed with 2% paraformaldehyde and immunostained with goat anti-Axl and mouse anti-FIV capsid. Findings shown in panels are representative experiments performed three independent times.